Chapter

Understanding the Drought Phenomenon in the Iberian Peninsula

Matilde García-Valdecasas Ojeda, Emilio Romero Jiménez, Sonia R. Gámiz-Fortis, Yolanda Castro-Díez and María Jesús Esteban Parra

Abstract

The analysis and understanding of drought phenomenon are essential for the management of hydrological resources. Drought indices are commonly used to predict these extreme events, being their suitability partly due to the use of climate fields at an adequate spatiotemporal resolution. This work aims to examine spatiotemporal patterns of drought over the Iberian Peninsula (IP), which is a region especially vulnerable to drought phenomenon. For this, climate data from a simulation completed with the Weather Research and Forecasting (WRF) model have been used. The spatiotemporal patterns of drought over the period 1980–2014 were examined using the Standardized Precipitation Evapotranspiration Index (SPEI) at the 3- and the 12-month time scales, and they were compared with other drought-related variables such as the surface evapotranspiration (SFCEVP), soil moisture (SM), and runoff. The results evidence that WRF is a valuable tool for characterizing droughts over the IP, providing large amounts of climate data at an adequate spatial resolution. Drought events seem to be more severe in regard to their duration over southern IP. Moreover, a good agreement between the SPEI at 3-month time scale with the SM and the SFCEVP is found. Additionally, the annual runoff evolves similarly to the SPEI at 12-month time scale.

Keywords: Weather Research and Forecasting model, regional climate models, drought indices, Standardized Precipitation Evapotranspiration Index, Iberian Peninsula

1. Introduction

Drought phenomenon has been considered as one of the major natural hazards causing numerous economic, social, and environmental losses [1]. In the context of ongoing global warming, an increase in frequency and intensity of this kind of extreme event is expected [2–4], and therefore, its accurate characterization is of high relevance for both mitigation and adaptation. In broad terms, drought is usually characterized as the scarcity of precipitation over a prolonged time period, but it is difficult to define and identify due to the great number of variables involved as well as the variety of sectors affected. Moreover, the characterization of the spatiotemporal

patterns of drought is very complex since it is very variable in space and time, this being particularly true in transitional zones such as the Iberian Peninsula (IP) [5].

In recent years, drought indices have been commonly used to identify, analyze, and monitor the occurrence of droughts. As indicated in [6], drought indices are variables based on climate information (e.g., precipitation, evapotranspiration, soil moisture, or runoff). They are used to analyze the effects of drought, allowing the definition of different drought characteristics (i.e., the duration and severity of droughts as well as the spatial extent). However, their accuracy strongly depends on long-term consistent climate data, and unfortunately, spatially and temporally regular climate observations are rare. In this context, the regional climate models (RCMs) are valuable tools providing climate information at an adequate spatiotemporal resolution to characterize regional drought patterns. In fact, drought phenomena are spatially complex, so detailed spatial scales are required in the study of droughts [7]. Additionally, Abatzoglou et al. [8] investigated the sensibility of drought indicators to the spatial resolution and found that the indices computed with the highest resolution explained over 10% more variability than those from coarser datasets.

Among different drought indices developed in recent years, the Standardized Precipitation Evapotranspiration Index (SPEI) [9] was proposed as an alternative to the Standardized Precipitation Index (SPI) [10]. Contrariwise to the SPI, the SPEI takes into account the effect of temperature for detecting droughts, and therefore, it seems to be more accurate in the context of global warming [11]. In fact, the increased global temperature trend is expected to increase the atmospheric evaporative demand, so regions, where the precipitation is normal in a given period (or even higher than normal), could be considered to suffer droughts. For instance, the role of the temperature is clear for the event occurred during summer 2003, which had devastating effects in central Europe mainly because of the anomalous temperatures in this period [9]. Furthermore, taking into account temperature data, this drought indicator has shown better performance than others based solely on precipitation (e.g., the SPI) for detecting droughts during summer, when the related impacts may become stronger [11].

This work investigates spatiotemporal patterns of drought through the SPEI to understand the drought temporal behavior over the IP, identifying those periods especially accused. This is of major relevance because the IP is characterized by highly variable and scarce precipitation leading to recurrent drought occurrences [12]. For this purpose, a 35-year climate simulation has been completed using the Weather Research and Forecasting (WRF) model [13] with the purpose of obtaining high-resolution climate data.

The chapter is structured as follows: Section 2 is devoted to detail the WRF model configuration as well as the statistical method applied to characterize the spatiotemporal patterns of droughts over the study region. Section 3 presents the main results regarding the temporal evolution of drought for the 35-year period (1980–2014), the identification of drought characteristics as well as the analysis of the relationships of the SPEI with other drought-related variables, such as the surface (actual) evapotranspiration, the soil moisture content, and the runoff. Finally, Section 4 summarizes the main conclusions obtained in this study.

2. Methodology

2.1 Climate input data

Hydroclimate variables at high spatiotemporal resolution were obtained by using the WRF-ARW model version 3.6.1. This RCM was run to simulate current climate characteristics over the IP and Balearic Islands (**Figure 1a**). The WRF model

was driven by the ECMWF ERA-Interim reanalysis data [14]. **Table 1** summarizes the main model setup used in this study. This configuration has been successfully used to represent the spatiotemporal patterns of droughts in the study region [15]. In [15], the authors analyzed the added value of using downscaled climate data to detect drought through the comparison with observational data and found that WRF provided a benefit with respect to its driving data in this regard.

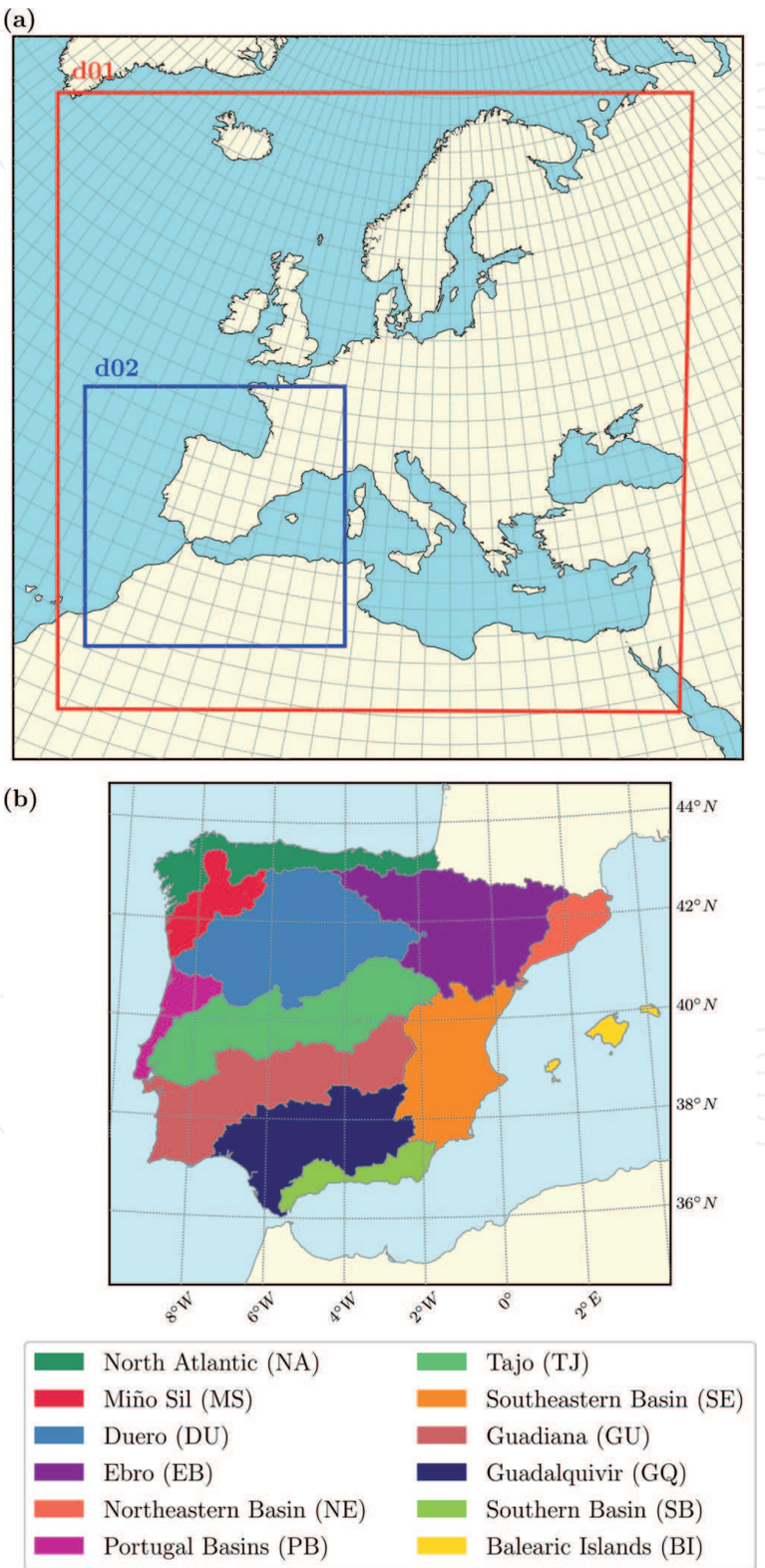

Figure 1.
(a) WRF domains: the EURO-CORDEX region (d01) at 0.44° of spatial resolution and the IP region (d02) with a spatial resolution of 0.088°, and (b) the main river basins over the IP.

Parameters	Description
Spatial configuration	Two "one-way" nested domains: (d01) EURO-CORDEX region at 0.44° (~50 km) of spatial resolution, and (d02) the IP at a spatial resolution of 0.088° (~10 km)
Temporal period	Period 1980–2014 with 11 months of spin-up
Vertical layer	41 vertical levels set the top of the atmosphere at 10 hPa
Nudging and sponge zone	Spectral nudging for waves above 600 km, only over the coarser domain and above the planetary boundary (PBL) Sponge zone: the 10 outer grid points of each domain
Physics schemes	Microphysics: WRF single-moment-3-class [16] Convection: Betts-Miller-Janjic [17, 18] PBL: convective asymmetric model version 2 [19] Land surface model: Noah LSM [20] Radiation: community atmosphere model 3.0 [21]

See [15] for more details.

Table 1.
The main model configuration.

In this study, the 3-hourly outputs in their native grid resolution have been used as climatic input data to analyze drought occurrences. In this way, the outputs of the WRF model at 10 km of spatial resolution (i.e., those from the inner domain d02, **Figure 1a**) were temporally aggregated at monthly scale, obtaining thus gridded long-term monthly climate data over land for the entire study region, for the period 1980–2014. The monthly variables used here are the averaged maximum and minimum temperature (Tmax and Tmin, respectively), the accumulated precipitation (pr), the accumulated surface evapotranspiration (SFCEVP), the mean soil moisture contained in the upper 1 m (SM), and the runoff. The WRF model, through the coupled Noah LSM scheme, contemplates two different runoff components, the surface and subsurface runoff. Here, the runoff was understood as the sum of these two components.

2.2 Defining drought occurrences over the Iberian Peninsula

2.2.1 The Standardized Precipitation Evapotranspiration Index (SPEI)

The SPEI has been widely used in recent years to characterize droughts, showing a good ability to detect, monitor, and analyze drought events [22–24]. This drought indicator is based on the SPI and differs in that it uses a simple "climatic water balance" instead of precipitation data in determining droughts. The temperature effect is indeed considered through the difference between the precipitation and the reference evapotranspiration (ET_0), this being aggregated at a range of time scales (1–48 months). Then, the aggregated climatic water balance is fitted to a statistical distribution, and subsequently, its probability density function is transformed into a random normal variable Z with mean of 0 and variance of 1. This latter assumption enables the comparison across regions by determining the probability of occurrence of a given drought event (**Table 2**). Thus, Z is the corresponding SPEI and indicates the number of standard deviations from the climatological mean. Therefore, and similar to the SPI, the SPEI is statistically robust, simple to compute and easily interpretable. Even more, the option to compute it at different time aggregations makes this index suitable for assessing different drought types (i.e., meteorological, agricultural, or hydrological droughts) [9].

In this study, the SPEI was computed at two different time aggregations: the 3- and 12-month time scales (hereinafter SPEI-03 and SPEI-12, respectively) using the SPEI R-package [25]. These time scales were chosen with the purpose of characterizing

SPEI value	Category	Probability (%)
SPEI ≥2	Extremely wet	2.3
2 ≥ SPEI >1.5	Severely wet	4.4
1.5 ≥ SPEI >1	Moderately wet	9.2
1 ≥ SPEI >0.5	Mildly wet	15.0
0.5 ≥ SPEI > −0.5	Nearly normal	38.2
−0.5 ≥ SPEI > −1.0	Mild drought	15.0
−1 ≥ SPEI > −1.5	Moderate drought	9.2
−1.5 ≥ SPEI > −2	Severe drought	4.4
SPEI < −2	Extreme drought	2.3

Table 2.
Drought categories and their probability of occurrence.

agricultural and hydrological droughts [6], respectively. Temporal series of the climatic water balance were obtained for the entire IP using the pr and the Tmax and Tmin from WRF at monthly scale. To approximate the ET_0, the Hargreaves equation [26] was used. Studies such as [27] evidenced that the Hargreaves method is able to approximate the ET_0 showing similar results to the Penman-Monteith equation [28] with the advantage that only temperature data are required to calculate it. The climatic water balance, here, is assumed to follow a log-logistic distribution [27]. This distribution has been used in many studies (e.g., [10, 27]) to fit the SPEI, mostly because it is a three-parameter distribution (i.e., negative values are permitted), which has been proved to better estimate the climatic water balance [27].

Then, the temporal series of SPEI at both 3- and 12-month time scales for each grid point were spatially averaged obtaining the SPEI evolution for each main river basin over the IP. Twelve main river basins were considered, as the result of aggregating smaller watersheds. They are North Atlantic (NA; composed by the Galician coast, the Western Cantabrian, and the Eastern Cantabrian watersheds), Miño-Sil (MS; the Miño-Sil, the Cávado, the Ave, and the Leça watersheds), Duero (DU), Ebro (EB), Northeastern Basins (NE), Portugal Basins (PB; the Vouga, Mondego, Lis, and Ribeiras do Oeste), Tajo (TJ), Southeastern Basins (SE), Guadiana (GU; Guadiana, Sado, Mira, and Ribeiras do Algarve), Guadalquivir (GQ; Guadalquivir, Tinto, Odiel, Piedras, Guadalete, and Barbate), Southern Basins (SB), and the Balearic Islands (BI) (**Figure 1b**).

In order to explore the severity of droughts, different drought characteristics have also been analyzed. For this, the established condition is that a dry event is occurring when at least two consecutive months are under the defined drought conditions. Therefore, a dry event was considered to begin when the SPEI falls below zero, and it ends when recovering positive values. Moreover, such a dry period is defined as drought if at least 1 month within the period reaches mild drought conditions (i.e., SPEI below −0.5 [29]). Then, the duration of droughts is understood as the number of months in each drought event. The intensity is the averaged value of the SPEI within the period expressed in absolute value. Additionally, the severity of the event (or minimum value reached) was also explored, which is expressed in terms of absolute value of the SPEI.

2.2.2 Temporal evolution of drought-related variables

Time series for each river basin from other drought-related variables were also examined. In this regard, the SM and SFCEVP were examined because they directly

affect the agricultural droughts. In fact, soil water availability is the major driver of the plant transpiration. To do this, the monthly time series of SM and SFCEVP were used to compute the standardized anomalies of such variables. These anomalies were computed with two purposes: (1) to remove seasonality and (2) to make the temporal evolutions comparable across regions. The SFCEVP was previously accumulated using 3-month time slices to also compare it with the SPEI-03, which is the time scale here used to characterize agricultural droughts.

On the other hand, to further investigate hydrological droughts, the temporal series of runoff, previously aggregated at annual scale, were used to compute the standardized anomalies series. This variable allows us to incorporate hydrological processes in drought characterization [6]. Hydrological droughts are developed slowly and persist longer than other forms of drought [30], so relationships between temporal series of runoff and the SPEI-12 must occur.

The relationship between such drought-related variables with the SPEI was investigated by computing temporal correlation coefficients for all river basins. Additionally, a t-test at the 95% confidence level was used to determine the significance of the correlation coefficients, previously considering the effect of the serial correlation by following the methodology proposed by Bretherton et al. [31].

3. Spatiotemporal patterns of droughts

3.1 Temporal evolution of the SPEI

This study begins with the analysis of the temporal evolution of the SPEI-03 and the SPEI-12 for all river basins over the entire study period (**Figure 2**). In the interest of clarity, SPEI evolution is represented according to the different drought categories (see **Table 2**). Concerning the SPEI-03 evolution (**Figure 2a**), the results showed a high temporal variability, which is a characteristic of meteorological droughts. That is, the SPEI changes frequently between drought and wet conditions. Furthermore, these results evidence the complexity of drought phenomena and therefore its characterization since very different conditions may be found in the different watersheds in a given moment (i.e., while certain river basins are affected by drought conditions, others presented normal or wet conditions). Several drought events were recorded over the study period. For instance, moderate to extreme drought conditions appeared during the years 1985, 1994–1995, 2005, and 2012 across a large part of the IP. Contrariwise, the years 1984, 1996–1998, 2003–2004 2010, and 2013 showed wet conditions over a large part of the IP.

Looking at the longest time scale (**Figure 2b**), the results presented a less variable behavior. In fact, for 12 months, the SPEI is less sensitive to variations from a given month, and hence, the changes between wet and dry conditions are less frequent and these are also longer. Moreover, the results display that, in general, dry and wet conditions are allocated in the same periods than those from the 3-month time scale, with the most severe droughts happening during 1995, 1999, 2005, and 2012. For these years, many watersheds were affected by severe drought conditions (i.e., SPEI below −2). Conversely, wet periods also appeared over many river basins during the years 1984, 1997, 2010, and 2013. Note the extreme wet conditions occurring during 2001 in the PB and the MS river basins.

3.2 Climatological characteristics of droughts

In order to further explore drought phenomenon, the duration distributions of drought events were explored for all river basins. **Figure 3** displays the box

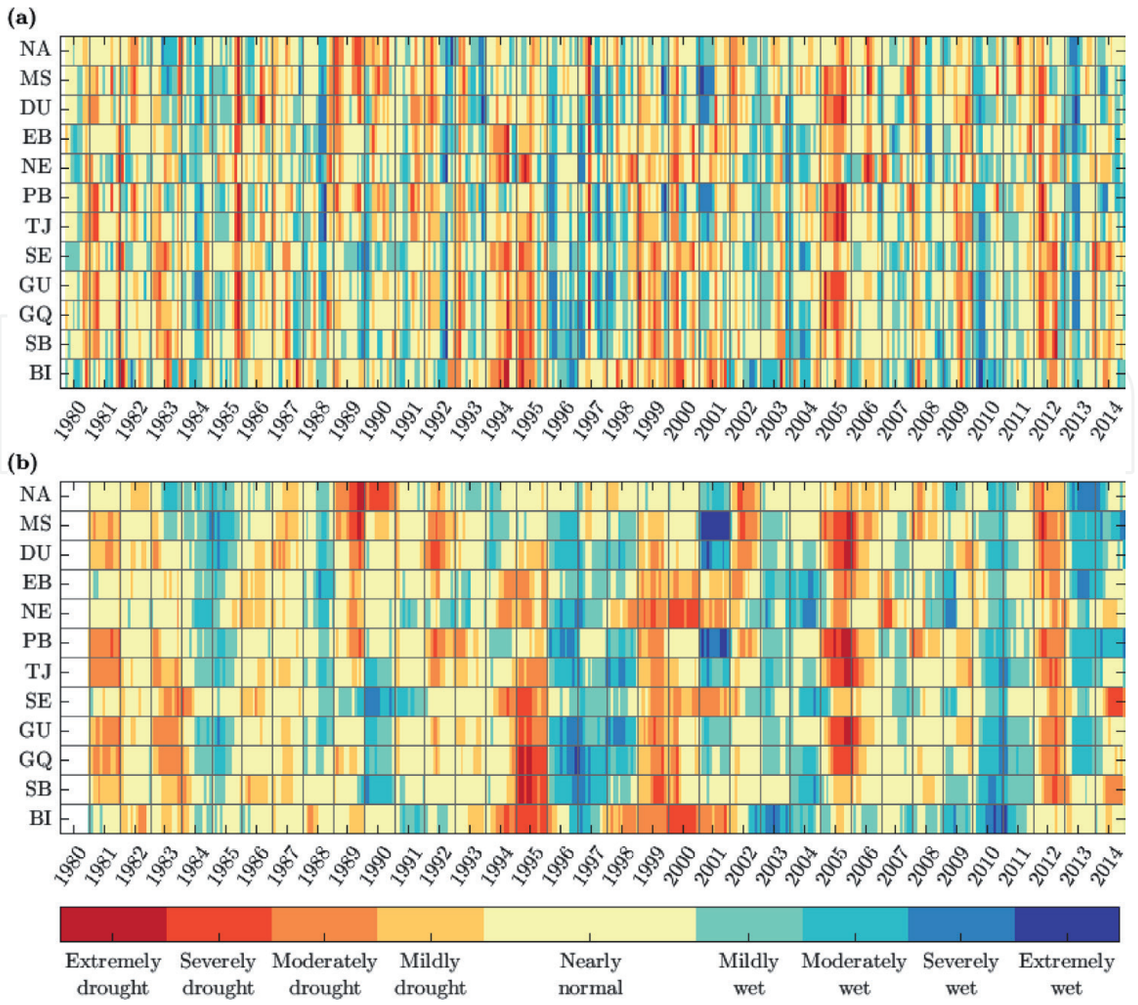

Figure 2.
Temporal evolution of the SPEI in all river basins between 1980 and 2014 at (a) 3- and (b) 12-month time scales. The color code is established according to the drought categories. Nomenclature: North Atlantic (NA), Miño-Sil (MS), Duero (DU), Ebro (EB), Northeastern Basins (NE), Portugal Basins (PB), Tajo (TJ), Southeastern Basins (SE), Guadiana (GU), Guadalquivir (GQ), Southern Basins (SB), and the Balearic Islands (BI).

plots of the duration of droughts for both the SPEI-03 and the SPEI-12 and for all river basins. This representation shows the scores of duration (in months) as well as their distributional characteristics. At 3 months (**Figure 3a**), the median was between 3 and 4 months, and the mean was around 4 months. Therefore, the mean was slightly higher than the median in all river basins, showing that the distributions are skewed to the right. The 97.5th percentile (limits of the upper whiskers) ranges from about 7.5 to 14.5 months, with the shortest and the longest durations occurring for the NE and the GQ river basins, respectively. On the other hand, the spread of the distribution is a signal of high variability in drought events, and it is marked by the size of the box (i.e., the interquartile range). In this regard, southern river basins (i.e., the TJ, SE, GU, GQ, and SB river basins) showed larger interquartile range than the northern ones (i.e., the NA, MS, DU, NE, and PB river basins).

For the SPEI-12 (**Figure 3b**), longer durations appeared for the period 1980–2014 in general, showing also more spread in their distributions. The median was between 5 and 14 months, reaching the maximum values again over the southern river basins. The mean duration of droughts was around 12 months, indicating that the mean was higher than the median in many cases. The 97.5th percentile was between 12 and 53 months with the highest one over the BI river basin. The major variability in terms of interquartile range seems to appear again over the BI river

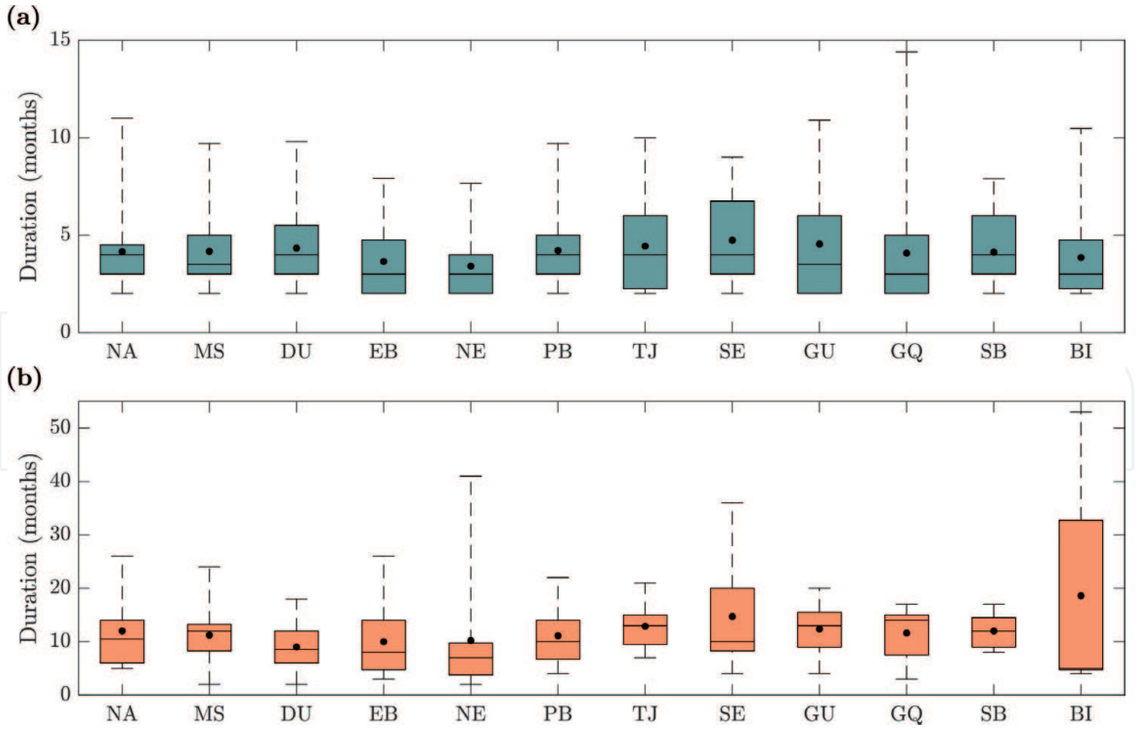

Figure 3.
Box plots of duration of drought events for all river basins, (a) for the SPEI-03 and (b) for the SPEI-12. The lower and upper parts of the boxes represent the 25th and the 75th percentiles, respectively; the line in the middle of each box is the median and the upper and lower whiskers indicate the 2.5th and 97.5th percentiles, respectively. The mean is displayed with black dots.

basin, which presented a large difference between the median and the third quartile (a difference of about 27 months). This latter feature reveals that most of the events for this period were short, but a longer event also occurred. The same behavior also appears in the SE river basins, but here the distribution is more homogenous, showing shorter events.

The box plots for the intensity of the drought events were also examined. In fact, the effects of drought phenomenon are stronger for longer events, but they are also the results of strong intensities. Hence, the distribution of the intensity has to be analyzed. In general, both time scales presented distributions with a low spread, particularly for those events from the SPEI-12. For the 3-month time scale (**Figure 4a**), the median was around 1 for all river basins, indicating that the events were, on average, moderate. As for duration, the mean was slightly higher than the median, reaching values of around 1.1. Concerning the extreme values, the 97.5th percentile was around 1.5 in general and reached a maximum above 1.7 (severe drought) over the EB and the PB river basins. Slightly lower medians are presented for events computed at 12 months (**Figure 4b**), where median intensities rise to values between 0.86 and 1.17 (i.e., from mild to moderate droughts). The mean values were around 1, and these were slightly higher than the median values in most of them. Some basins as MS, EB, or PB presented the opposite behavior. Concerning the extreme values in terms of intensity, the 97.5th percentile was also slightly lower than for the previous time scale (values around 1.45), reaching values above 1.5 over the GQ, the SB, and the PB river basins.

In addition, to examine trends of drought occurrences along the study period, the duration, intensity, and severity of drought events were analyzed by computing such parameters in two different periods: 1980–1999 and 2000–2014. Then, the median changes between both periods in the three parameters were used to develop a categorical classification.

Figure 5 displays the trends for the main river basins and for both time scales. At 3 months (left map), different behaviors were shown. The DU river basin has a positive trend in the three parameters, and the EB presented the opposite behavior. Intermediate trends appeared in the rest of the IP, showing watersheds where a positive trend occurred only in the median severity (i.e., the MS and the SE river basins). In other watersheds, the positive trend only appeared in the median intensity (i.e., the NE, the BI, and GQ river basins), but there were also watersheds with an increase in two of the characteristics analyzed. However, for the 12-month time scale (right

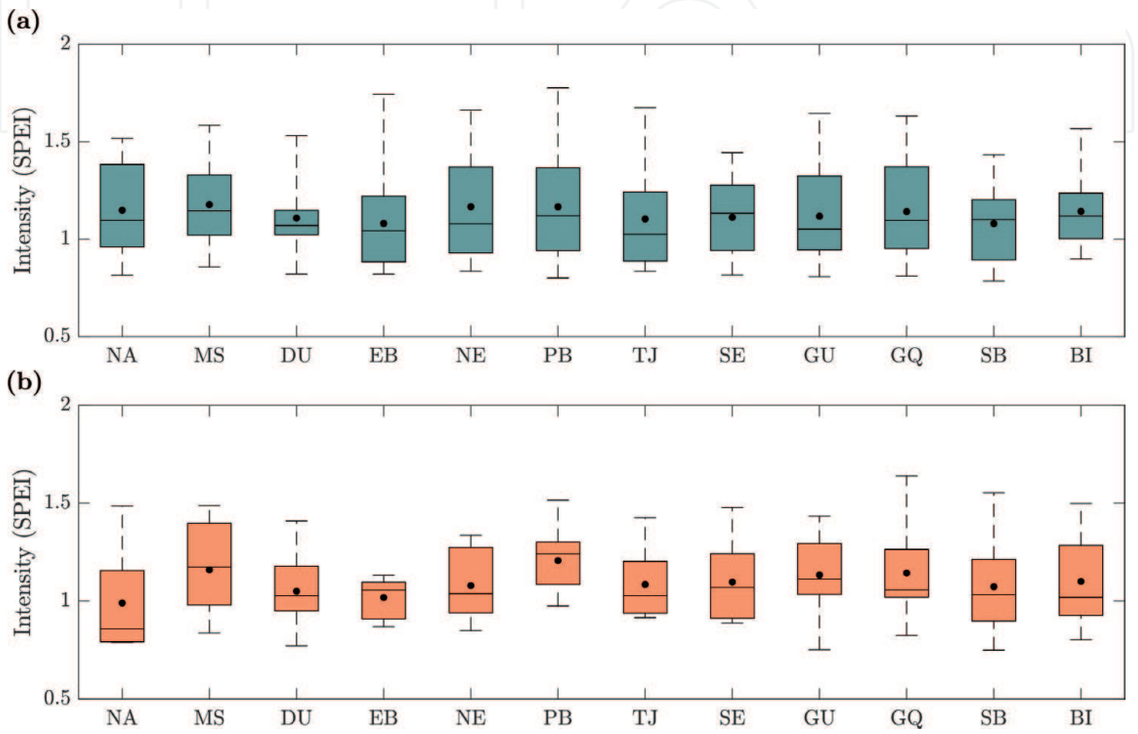

Figure 4.
Box plots of intensity of drought events for all river basins, (a) for the SPEI-03 and (b) for the SPEI-12. The lower and upper parts of the boxes represent the 25th and the 75th percentiles, respectively; the line in the middle of each box is the median and the upper and lower whiskers indicate the 2.5th and 97.5th percentiles, respectively. The mean is displayed with black dots.

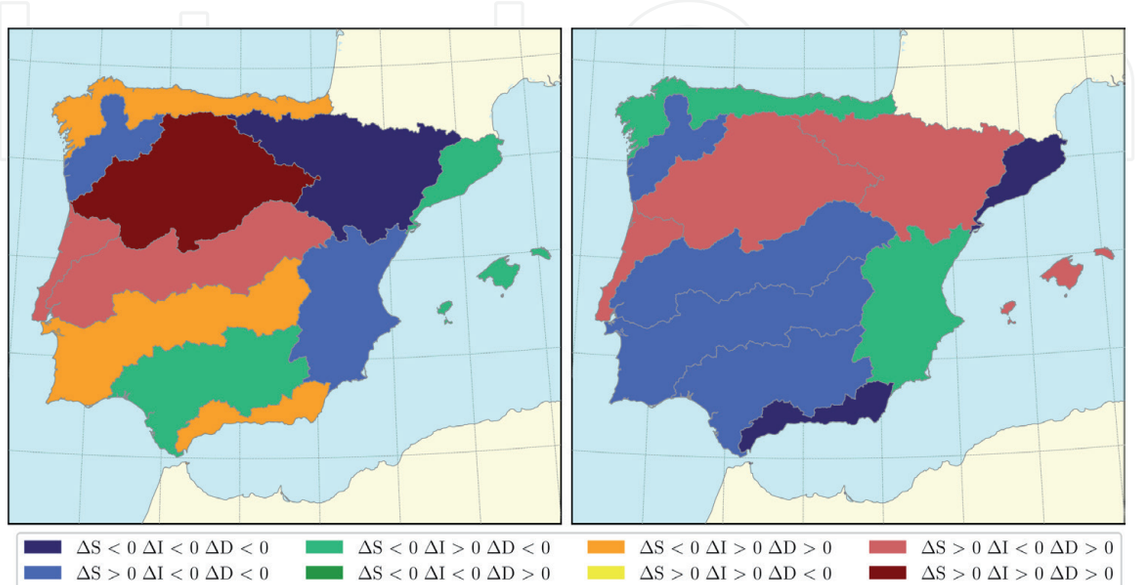

Figure 5.
Categorical classification of droughts for the SPEI-03 (left) and the SPEI-12 (right) based on the changes in severity (ΔS), intensity (ΔI), and duration (ΔD) between the periods 1980–1999 and 2000–2014.

map), the positive trends are less frequent, showing an increased trend in more than one parameter only for the PB, the DU, and the EB river basins. In these three basins, the results showed an increase in both severity and duration of drought events.

4. Temporal evolution of drought-related variables

Finally, we investigated the relationship between the SPEI and other drought-related variables. **Figure 6** shows the temporal evolution of the standardized anomalies of SFCEVP accumulated at 3 months as well as of the monthly mean SM for all river basins. The SPEI-03 was also displayed with comparative purposes. In broad terms, the SM evolves similar to the SPEI-03, showing correlations above 0.7 in all river basins (second column in **Table 3**). However, the SFCEVP presents more

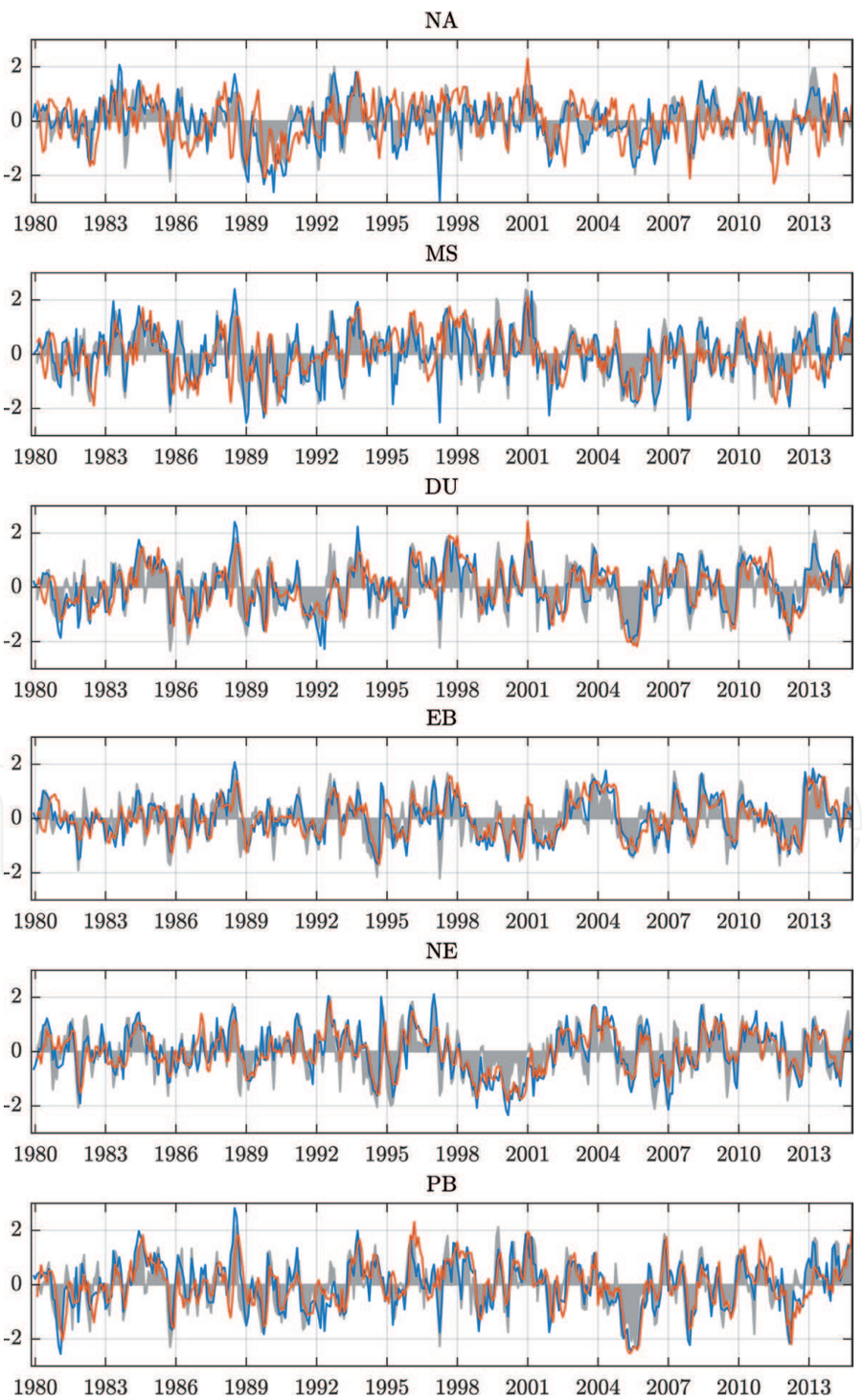

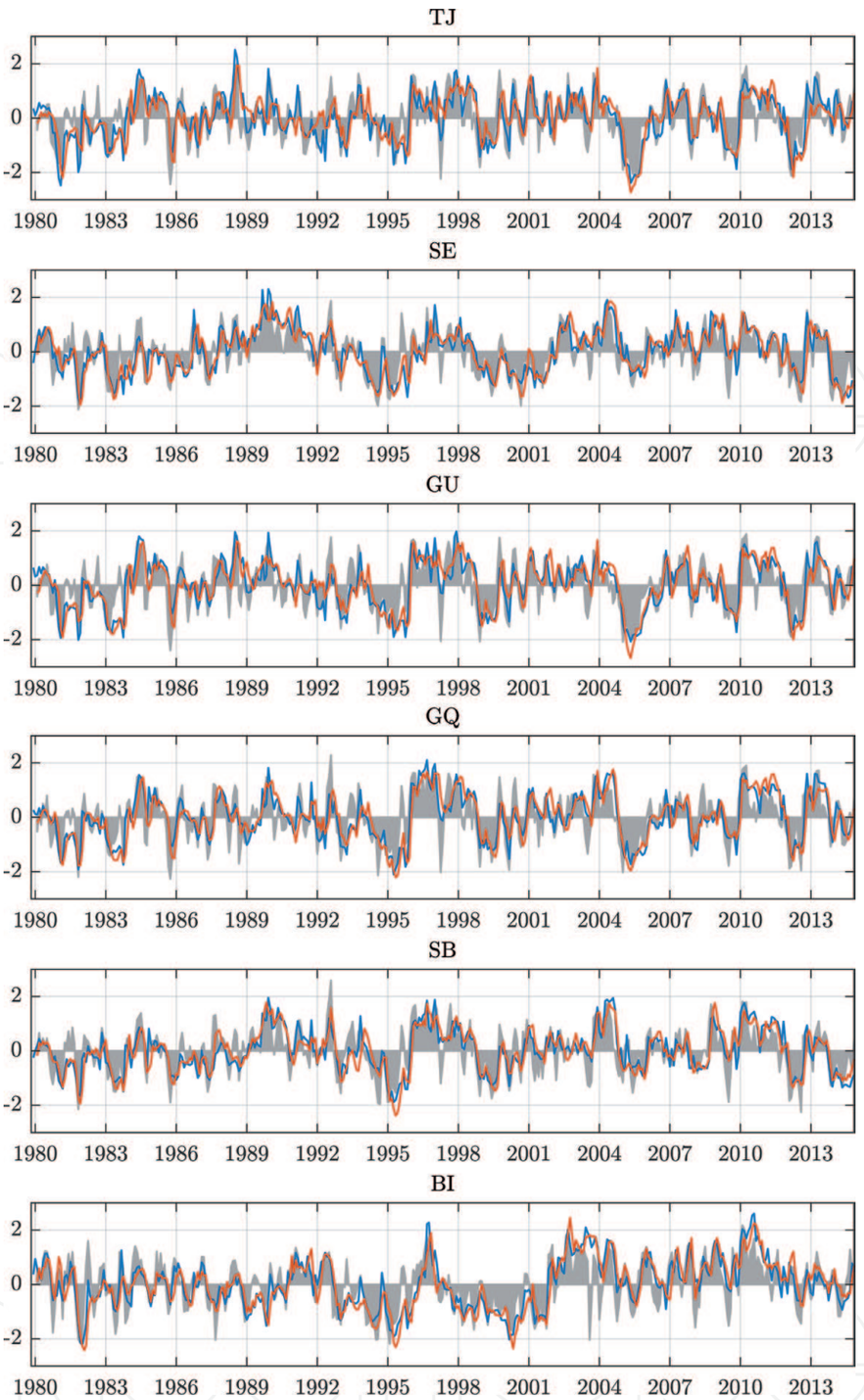

Figure 6.
Standardized anomalies of the 3 months accumulated SM (blue line) and SFCEVP (orange line), SPEI-03 (gray area) evolutions for the NA, MS, DU, EB, NE, PB, TJ, SE, GU, GQ, SB, and BI river basins.

River basins	SPEI-SM	SPEI-SFCEVP	SPEI-runoff
NA	0.85*	0.24	0.91*
MS	0.84*	0.49*	0.91*
DU	0.82*	0.56*	0.80*
EB	0.81*	0.53*	0.80*
NE	0.81*	0.67*	0.80*
PB	0.84*	0.60*	0.87*

River basins	SPEI-SM	SPEI-SFCEVP	SPEI-runoff
TJ	0.79*	0.56*	0.84*
SE	0.80*	0.70*	0.80*
GU	0.76*	0.60*	0.80*
GQ	0.77*	0.61*	0.81*
SB	0.75*	0.67*	0.81*
BI	0.76*	0.63*	0.77*

*Significant correlations at 95% confidence level.

Table 3.
Pearson's temporal correlation (r) between the SPEI-03 and the soil moisture content (SPEI-SM) and SFCEVP (SPEI-SFCEVP), and between the SPEI-12 and the 12 months' accumulated runoff (SPEI-runoff).

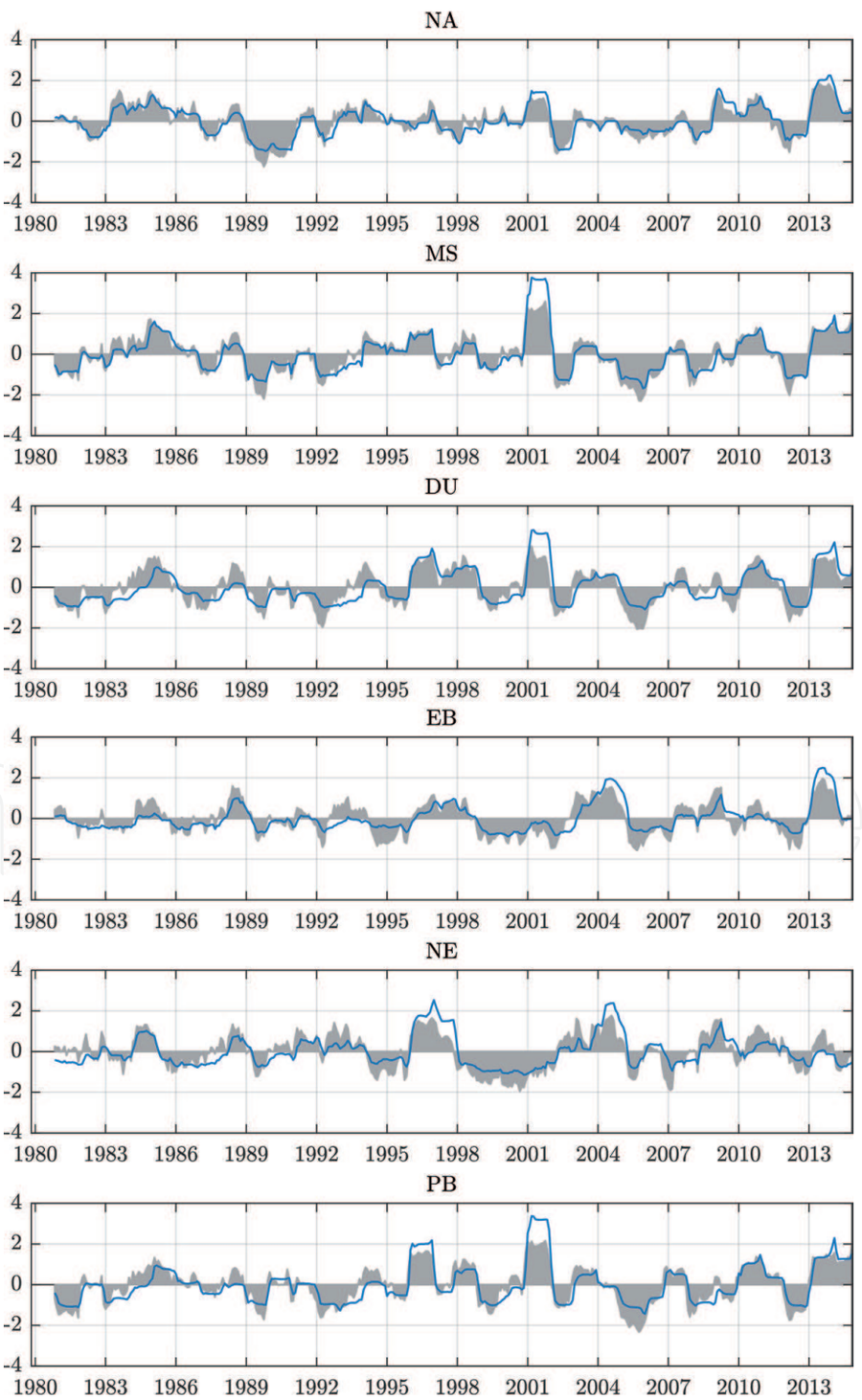

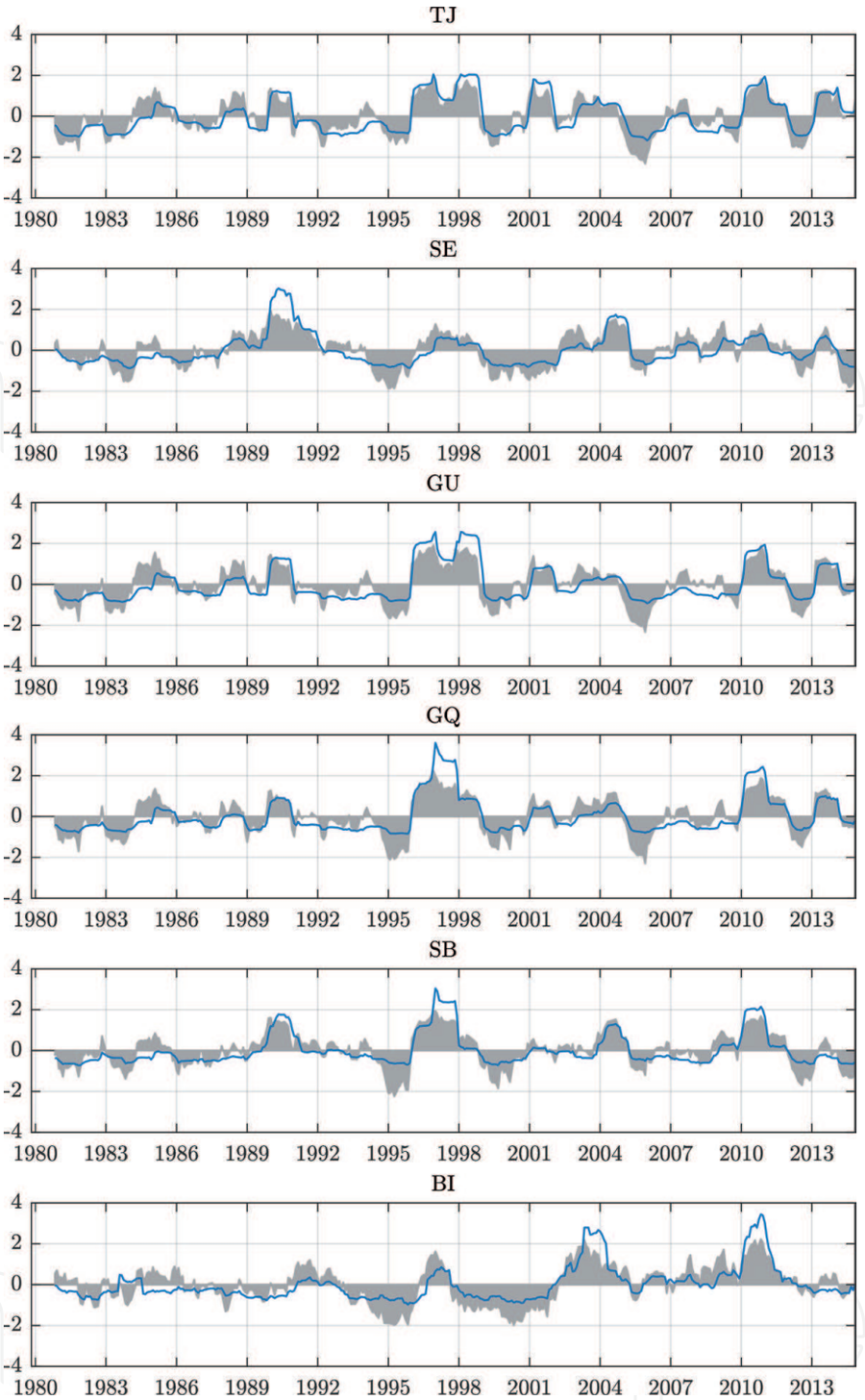

Figure 7.
Standardized anomalies of the 12 months accumulated runoff (blue line) and the SPEI-12 (gray area) temporal series for NA, MS, DU, EB, NE, PB, TJ, SE, GU, GQ, SB, and BI river basins.

discrepancies, especially for the NA and the MS river basins. This latter is probably produced because wet zones such as the northwestern IP are characterized by a SFCEVP less sensitive to changes in SM, being energy-limited regions. Here, only under very long periods of precipitation scarcity, the SFCEVP is strongly affected by the water availability. Contrariwise, in transitional zones (i.e., southern IP), the SFCEVP is usually limited, and then, the SM, and consequently the precipitation, largely controls the SFCEVP. In this region (e.g., the GQ or the SE river basins), the SFCEVP agrees really well with the SPEI-03. This behavior is reflected in the temporal correlations between the SFCEVP and the SPEI-03 (third column in **Table 3**), which tends to be higher over the southern river basins. In broad terms, the Pearson's

correlations also show that the SPEI-03 correlates well in general with the SFCEVP, showing significant correlations at the 95% confidence level for all river basins, except over the NA river basins.

The hydrological droughts are represented in **Figure 7**. Here, the temporal evolution of the runoff, which was obtained by aggregated standardized anomalies at 12 months, was displayed, as well as the SPEI-12. As for the previous analysis, different periods with positive and negative anomalies were recorded in all river basins, reproducing wet and dry periods similar to the SPEI-12. In fact, the SPEI-12 reflects long-term precipitation patterns, being thus useful to determine streamflow and reservoir levels. For instance, a marked wet period clearly appeared during 2001 over the NA, the MS, the DU, the PB, and the TJ river basins in both the runoff and the SPEI-12 temporal series. In the same way, certain river basins presented marked negative standardized anomalies of runoff during 2005, which also showed important negative values of SPEI-12. As expected, r between the SPEI-12 and the runoff was really high showing values around 0.85, with the highest ones over the NA and the MS river basins (r values of 0.91).

5. Conclusions

This chapter is devoted to analyzing spatiotemporal patterns of droughts over the IP, a region particularly vulnerable to this extreme event [7] for the period 1980–2014. To do this, a regional climate simulation using the WRF model was completed, obtaining thus high spatiotemporal resolution climate data. Temperature and precipitation data from WRF were used to compute the SPEI at 3- and 12-month time scales with the purpose of analyzing different drought applications (e.g., agricultural and hydrological). This index has proved to be adequate to analyze droughts in the context of global warming.

Firstly, the regional performance of the SPEI was assessed. The most general evolution in droughts is consistent with other studies that allocated the main drought episodes occurred over the IP (e.g., [27]). The results evidenced that WRF appears as a promising tool for analyzing droughts since they provide a great number of climate variables at adequate spatial and temporal resolutions, which are unusually obtained from observations. In fact, climate data from regional simulations may be useful to determine where and when drought is occurring, providing valuable information to compute different drought indices using different drought-related variables.

These results also show that the SPEI-03 represents more frequent and shorter episodes, with the median duration and intensity of about 3–4 months and 1, respectively. In this regard, the largest events occurred over the southern IP, which is especially vulnerable due to its aridity conditions. In fact, this region is arid and then major damages may be produced under the occurrence of severe drought events.

On the other hand, the SPEI-12 presented longer drought episodes, showing, in general, more spread in its duration distributions, with the median values ranging from 5 to 17 months. However, in regard to the intensity, droughts presented similar behavior for both time scales.

Concerning the existence of the trends in droughts along the analyzed period, the results indicate that, in general, an increase in at least one of the drought properties occurred over the period 2000–2014 with respect to the period 1980–1999 in most of the river basins, more evident for the SPEI-03.

In the comparison between the SM and the SPEI-03, the results show that this variable presents a good agreement with the SPEI, which is an index based on a balance between water supply and potential demand at 3 months, which suggests

that the 3-month time scale is adequate to study agricultural drought in general over the IP. In fact, it is well known that variations in the SM are the result of changes in precipitation, SFCEVP, and runoff. Therefore, it is an accumulated measure of water availability, and thus, it can be used to detect dry and wet periods [32]. On the other hand, the SFCEVP also affects the agricultural systems, but its relationship with droughts is more complex. That is, the SFCEVP is the actual loss of water, which depends on the water demand by plants and the atmosphere (i.e., the potential evapotranspiration and consequently the temperature), but also on the water availability. This is clearly shown in arid regions, in which the SM largely controls the SFCEVP. Therefore, the actual water balance can be used as a proxy of drought occurrences, but it must be interpreted with caution in regions in which the SFCEVP is not a limiting factor such as the northwestern IP.

Hydrological droughts can be defined as the scarcity of surface and subsurface water resources that leads to negative effects in water resources management system. In this regard, our results indicate that the annual runoff seems to be a good variable to identify hydrological droughts, showing an especial good agreement with the SPEI-12.

The agreement between variables shown here also evidences that the SPEI is an adequate index to investigate drought conditions over the IP, reproducing these in a similar way than other drought-related variables over the study period. This is of high relevance to adequately develop strategies to mitigate the effects of droughts in the future.

Acknowledgements

This study has been financed by the Spanish Ministry of Economy and Competitiveness, with additional support from the European Community fund (FEDER), project CGL2013-48539-R and CGL2017-89836-R. The WRF simulation was run in the ALHAMBRA supercomputer infrastructure (https://alhambra.ugr.es). The ERA-Interim data were obtained from ECMWF portal and the WRF model from NCAR.

Conflict of interest

The authors declare that the research was conducted in absence of any potential conflict of interest.

Author details

Matilde García-Valdecasas Ojeda*, Emilio Romero Jiménez, Sonia R. Gámiz-Fortis, Yolanda Castro-Díez and María Jesús Esteban Parra
Department of Applied Physics, University of Granada, Granada, Spain

*Address all correspondence to: mgvaldecasas@ugr.es

References

[1] Whilite DA. Drought as a natural hazard: Concepts and definitions. In: Whilite DA, editor. Drought: A Global Assessment. London: Routledge; 2010. pp. 3-18

[2] Sheffield J, Wood EF. Projected changes in drought occurrence under future global warming from multi-model, multi-scenario, IPCC AR4 simulations. Climate Dynamics. 2008;**31**:79-105. DOI: 10.1007/s00382-007-0340-z

[3] Dai A. Drought under global warming: A review. Wiley Interdisciplinary Reviews: Climate Change. 2011;**2**:45-65. DOI: 10.1002/wcc.81

[4] Wang K, Dickinson RE, Liang S. Global atmospheric evaporative demand over land from 1973 to 2008. Journal of Climate. 2012;**25**:8353-8361. DOI: 10.1175/JCLI-D-11-00492.1

[5] Vicente-Serrano SM. Spatial and temporal analysis of droughts in the Iberian Peninsula (1910-2010). Hydrological Science Journal. 2006;**51**:83-97. DOI: 10.1623/hysj.51.1.83

[6] Mishra AK, Singh VP. A review of drought concepts. Journal of Hydrology. 2010;**391**:202-216. DOI: 10.1016/j.jhydrol.2010.07.012

[7] Vicente-Serrano SM, Cuadrat-Prats JM. Trends in drought intensity and variability in the middle Ebro valley (NE of the Iberian Peninsula) during the second half of the twentieth century. Theoretical and Applied Climatology. 2007;**88**:247-258. DOI: 10.1007/s00704-006-0236-6

[8] Abatzoglou JT, Barbero R, Wolf JW, Holden ZA. Tracking interannual streamflow variability with drought indices in the US Pacific Northwest. Journal of Hydrometeorology. 2014;**15**:1900-1912. DOI: 10.1175/JHM-D-13-0167.1

[9] Vicente-Serrano SM, Beguería S, López-Moreno JI. A multiscalar drought index sensitive to global warming: The standardized precipitation evapotranspiration index. Journal of Climate. 2010;**23**:1696-1718. DOI: 10.1175/2009JCLI2909.1

[10] McKee TB, Doesken NJ, Kleist J. The relationship of drought frequency and duration to time scales. In: Proceedings of the 8th Conference on Applied Climatology; 17 January 1993. Boston, MA: American Meteorological Society; 1993. pp. 179-183

[11] Vicente-Serrano SM, Beguería S, Lorenzo-Lacruz J, Camarero JJ, López-Moreno JI, Azorin-Molina C, et al. Performance of drought indices for ecological, agricultural, and hydrological applications. Earth Interactions. 2012;**16**:1-27. DOI: 10.1175/2012EI000434.1

[12] Vicente-Serrano SM, Lopez-Moreno JI, Beguería S, Lorenzo-Lacruz J, Sanchez-Lorenzo A, García-Ruiz JM, et al. Evidence of increasing drought severity caused by temperature rise in southern Europe. Environmental Research Letters. 2014;**9**:044001. DOI: 10.1088/1748-9326/9/4/044001

[13] Skamarock WC, Klemp JB, Dudhia J, Gill DO, Barker DM, Duda MG, et al. A Description of the Advanced Research WRF Version 3, NCAR Technical Note. Boulder, Colorado, USA: Mesoscale and Microscale Meteorology Division. National Center for Atmospheric Research; 2008

[14] Dee DP, Uppala SM, Simmons AJ, Berrisford P, Poli P, Kobayashi S, et al. The ERA-interim reanalysis: Configuration and performance of the data assimilation system. Quarterly

Journal of the Royal Meteorological Society. 2011;**137**:553-597. DOI: 10.1002/qj.828

[15] García-Valdecasas Ojeda M, Gámiz-Fortis SR, Castro-Díez Y, Esteban-Parra MJ. Evaluation of WRF capability to detect dry and wet periods in Spain using drought indices. Journal of Geophysical Research: Atmospheres. 2017;**122**:1569-1594. DOI: 10.1002/2016JD025683

[16] Hong SY, Dudhia J, Chen SH. A revised approach to ice microphysical processes for the bulk parameterization of clouds and precipitation. Monthly Weather Review. 2004;**132**:103-120. DOI: 10.1175/1520-0493(2004)132<0103:ARATIM>2.0.CO;2

[17] Betts AK, Miller MJ. A new convective adjustment scheme. Part II: Single column tests using GATE wave, BOMEX, ATEX and arctic air-mass data sets. Quarterly Journal of the Royal Meteorological Society. 1986;**112**: 693-709. DOI: 10.1002/qj.49711247308

[18] Janjić ZI. The step-mountain coordinate: Physical package. Monthly Weather Review. 1990;**118**:1429-1443. DOI: 10.1175/1520-0493(1990)118<1429:TSMCPP>2.0.CO;2

[19] Pleim JE. A combined local and nonlocal closure model for the atmospheric boundary layer. Part I: Model description and testing. Journal of Applied Meteorology and Climatology. 2007;**46**:1383-1395. DOI: 10.1175/JAM2539.1

[20] Chen F, Dudhia J. Coupling an advanced land surface—Hydrology model with the Penn State—NCAR MM5 modeling system. Part I: Model implementation and sensitivity. Monthly Weather Review. 2001;**129**: 569-585. DOI: 10.1175/1520-0493(2001)129<0569:CAALSH>2.0.CO;2

[21] Collins WD, Rasch PJ, Boville BA, Hack JJ, McCaa JR, Williamson DL, et al. Description of the NCAR Community Atmosphere Model (CAM 3.0). NCAR Technical Note NCAR/TN-464+ STR; 2004. p. 226

[22] Kim BS, Chang IG, Sung JH, Han HJ. Projection in future drought hazard of South Korea based on RCP climate change scenario 8.5 using SPEI. Advances in Meteorology. 2016;**2016**(4148710):1-23. DOI: 10.1155/2016/4148710

[23] Wang W, Ertsen MW, Svoboda MD, Hafeez M. Propagation of drought: From meteorological drought to agricultural and hydrological drought. Advances in Meteorology. 2016;**2016**(6547209):1-5. DOI: 10.1155/2016/6547209

[24] Meque A, Abiodun BJ. Simulating the link between ENSO and summer drought in southern Africa using regional climate models. Climate Dynamics. 2015;**44**:1881-1900. DOI: 10.1007/s00382-014-2143-3

[25] Beguería S, Vicente-Serrano SM. SPEI: Calculation of the Standardized Precipitation-Evapotranspiration Index. R Package Version. 2013. p. 1. Available from: http://cran.r-project.org/package=SPEI

[26] Hargreaves GH. Defining and using reference evapotranspiration. Journal of Irrigation and Drainage Engineering. 1994;**120**:1132-1139. DOI: 10.1061/(ASCE)0733-9437(1994)120%3A6(1132)

[27] Beguería S, Vicente-Serrano SM, Reig F, Latorre B. Standardized precipitation evapotranspiration index (SPEI) revisited: Parameter fitting, evapotranspiration models, tools, datasets and drought monitoring. International Journal of Climatology. 2014;**34**:3001-3023. DOI: 10.1002/joc.3887

[28] Allen RG, Pereira LS, Raes D, Smith M. Crop Evapotranspiration-Guidelines for Computing Crop Water Requirements. FAO Irrigation and Drainage Paper 56. Rome: FAO; 1998. 300:D05109

[29] Y-j L, Zheng X-d, Lu F, Ma J. Analysis of drought evolvement characteristics based on standardized precipitation index in the Huaihe River basin. Procedia Engineering. 2012;**28**:434-437. DOI: 10.1016/j.proeng.2012.01.746

[30] Keyantash J, Dracup JA. The quantification of drought: An evaluation of drought indices. Bulletin of the American Meteorological Society. 2002;**83**:1167-1180. DOI: 10.1175/1520-0477-83.8.1167

[31] Bretherton CS, Widmann M, Dymnikov VP, Wallace JM, Bladé I. The effective number of spatial degrees of freedom of a time-varying field. Journal of Climate. 1999;**12**:1990-2009. DOI: 10.1175/1520-0442(1999)012<1990:TENOSD>2.0.CO;2

[32] Sheffield J, Wood EF. Global trends and variability in soil moisture and drought characteristics, 1950-2000, from observations-driven simulations id the terrestrial water cycle. Journal of Climate. 2008;**21**:432-458. DOI: 10.1175/2007JCLI1822.1